



Metal triflates formation of C12-C22 phenolic compounds by simultaneous C-O breaking and C-C coupling of lignin-derived benzyl phenyl ether

Journal:	<i>Dalton Transactions</i>
Manuscript ID	DT-ART-06-2021-002136.R2
Article Type:	Paper
Date Submitted by the Author:	22-Oct-2021
Complete List of Authors:	Rahaman, Mohammad Shahinur; University of Louisville, Chemical Engineering Tulaphol, Sarttrawut; University of Louisville, Chemical Engineering; Thammasat University, Chemical engineering; King Mongkut's University of Technology Thonburi, Chemistry molley, ashten; University of Louisville, Mills, Kyle; University of Louisville Hossain, Anwar; University of Louisville, Chemical Engineering Yelle, Daniel; USDA Forest Service Maihom, Thana; Kasetsart University Kamphaeng Saen Campus, Department of Chemistry, Faculty of Liberal Arts and Science Sathitsuksanoh, Noppadon; University of Louisville, Chemical Engineering

1 **Metal triflates formation of C₁₂-C₂₂ phenolic compounds by simultaneous C-O breaking and C-C**
2 **coupling of benzyl phenyl ether**

3 Mohammad Shahinur Rahaman¹, Sarttrawut Tulaphol², Ashten Molley¹, Kyle Mills¹, Md. Anwar
4 Hossain¹, Daniel Yelle³, Thana Maihom⁴, Noppadon Sathitsuksanoh^{1*}

5 ¹Department of Chemical Engineering, University of Louisville, Louisville, KY 40292, USA

6 ²Sustainable Polymer & Innovative Composite Materials Research Group, Department of Chemistry,
7 Faculty of Science, King Mongkut's University of Technology Thonburi, Bangkok10140, Thailand

8 ³USDA, Forest Products Laboratory, Madison, WI, 53726, USA

9 ⁴Department of Chemistry, Faculty of Liberal Arts and Science, Kasetsart University, Kamphaeng
10 Saen Campus, Nakhon Pathom 73140, Thailand

11 * Corresponding author: N.sathitsuksanoh@louisville.edu

12

13 **Abstract**

14 Catalytic pathways to produce high carbon number compounds from benzyl phenyl ether
15 require multiple steps to break the aryl etheric carbon-oxygen bonds; these steps are followed
16 by energy-intensive processes to remove oxygens and/or carbon-carbon coupling. Here we
17 show an upgrading strategy to transform benzyl phenyl ether into large phenolic (C₁₂-C₂₂)
18 compounds by a one-step C-O breaking and C-C coupling catalyzed by metal triflates under a
19 mild condition (100°C and 1 bar). Hafnium triflate was the most selective for the desired
20 products. In addition, we measured the effect of solvent polarity on the catalytic performance.
21 Solvents with a polarity index less than 3.4 promoted the catalytic activity and selectivity to C₁₂-
22 C₂₂ phenolic products. These C₁₂-C₂₂ phenolic compounds have potential applications for phenol-
23 formaldehyde polymers, diesel/jet fuels, and liquid organic hydrogen carriers.

24

25

26

27 **Keywords.** Metal triflates; hafnium; lignin, diesel, jet, liquid organic hydrogen carriers; Fries
28 rearrangement; solvent effect

29 Introduction

30 The development of chemical conversion strategies for lignin is important for production of fuels and
31 chemicals from renewable plant lignocellulose.^{1, 2} Lignin may account for as much as 35 wt% of the
32 total lignocellulosic biomass. Lignin is a highly branched polymer composed of hydroxy- and methoxy-
33 substituted phenylpropane (C₃C₆) units joined by carbon-carbon (C-C) and ether (C-O) linkages. The
34 C-O linkages are abundant in lignin, including β-O-4, α-O-4, and 4-O-5.³⁻⁵ The relative ratio of these
35 linkages in lignin depends on plant species (**Table S1**). In general, most current lignin conversion
36 strategies start from depolymerization (hydrolysis or pyrolysis) to produce lignin fragments,
37 i.e., C₆-C₉ phenolic compounds.^{6, 7} Then, the phenolic compounds undergo
38 hydrodeoxygenation and/or hydrogenation to produce C₆-C₉ hydrocarbons, suitable for
39 gasoline.

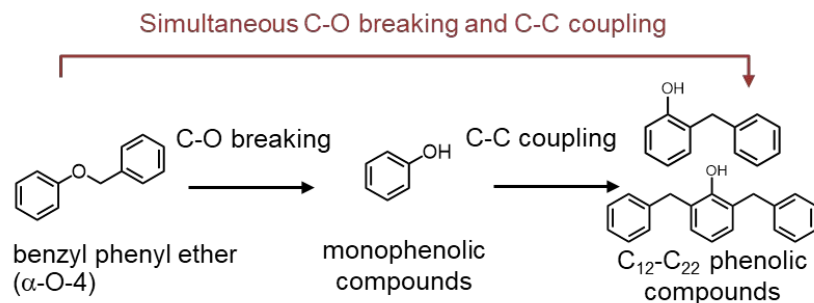
40

41 Although low carbon number phenolic compounds are readily obtainable from lignin, the use
42 of lignin biomass would be greatly stimulated by the availability of an efficient route to
43 transform lignin into higher carbon phenolic compounds (C₁₂-C₂₂) as precursors for diesel- and
44 jet-range fuels.^{7, 8} We can increase carbon number by using C-C coupling reactions with lignin-derived
45 monomers.⁸ For example, Zhang et al.⁹ and Bi et al.¹⁰ performed a cascade of pyrolysis of
46 sawdust/lignin into low-carbon phenolics, followed by alkylation of these low-carbon phenolics by the
47 ionic liquid [C₄C₁im]Cl-2AlCl₃ (1-butyl-3-methylimidazolium chloroaluminate) into C₈-C₁₅
48 phenolics. The combined C-C coupling and hydrodeoxygenation of phenol and substituted phenols to
49 yield bi-cycloalkanes (i.e., C₁₂-C₁₈) can be achieved using a cascade reaction over Pd nanoparticles on
50 acidic support at 200°C and 50 bar H₂.¹¹ These approaches are effective, but there are two major
51 impediments to the transformation of lignin and its fragments to C₁₂-C₂₂ phenolic compounds: (1)
52 severe depolymerization conditions¹² because of the high stability of the aryl etheric C-O
53 bonds,^{13, 14} and (2) multiple reaction steps (C-O breaking and C-C coupling) required to produce
54 larger chemical precursors (C₁₂-C₂₂ phenolic compounds)⁸ as depicted in **Scheme 1**. These challenges
55 contribute to the production cost and retard the adoption of developed technology.

56

57

58



59

60 **Scheme 1.** Transformation pathways for benzyl phenyl ether (α -O-4) into C₁₂-C₂₂ phenolic
61 compounds.

62

63 Here, we describe a direct transformation of benzyl phenyl ether by simultaneous C–O bond
64 breaking and C-C coupling catalyzed by metal triflates in a liquid phase reaction. Hafnium triflate
65 was the most active and selective catalyst to produce desired C₁₂-C₂₂ phenolic products in
66 solvents with a polarity index lower than 3.4. Our findings establish a new, more efficient
67 upgrading route for lignin model compounds.

68

69 **Materials and Methods**

70 **Materials.** Benzyl phenyl ether (98 wt.%, Sigma-Aldrich, St. Louis, MO, USA), 2-phenethyl phenyl
71 ether (99 wt.%, Frinton Laboratories, Inc., Hainesport, NJ, USA), and diphenyl ether (99 wt.%, Sigma-
72 Aldrich) were used as received unless noted otherwise. *n*-Heptane (99 wt.%, Beantown Chemical)
73 and *n*-dodecane (≥ 99 wt.%, Beantown Chemical) were used as a solvent, and internal standard,
74 respectively, unless noted otherwise. Metal triflates, La(OTf)₃, Al(OTf)₃, Ti(OTf)₄, Zn(OTf)₂, Yb(OTf)₃,
75 Y(OTf)₃, Er(OTf)₃, Sc(OTf)₃, Fe(OTf)₃, and Hf(OTf)₄, were purchased from commercial supplier and
76 used as received unless noted otherwise. These anhydrous metal triflates were stored in desiccators.
77 All chemicals were used as received unless otherwise noted. Their CAS numbers, purity, and
78 manufacturers are listed in **Table S2**.

79

80 **Catalysis testing.** Reactions were conducted with solutions of benzyl phenyl ether in *n*-heptane and
81 *n*-dodecane with a ratio of feed:*n*-heptane:dodecane = 1.0:8.5:0.5 by weight. Heptane was the
82 reaction solvent; dodecane was added as the internal standard for quantifying conversion and
83 product yields. The catalyst was 20 mol% of metal with respect to the benzyl phenyl ether feed. The

84 catalysts were loaded in a glove box to minimize the effect of moisture on the activity of the metal
85 triflates. The reaction mixture was stirred at 100°C in a pressure vessel (Ace Glass Inc., Vineland, NJ,
86 USA) containing a small magnetic stir bar and sealed using a polytetrafluoroethylene/silicone septa
87 and metal crimp top. The sealed reactor was placed in a temperature-controlled silicon oil bath on a
88 magnetic stir plate, and samples were taken at various times. The products were analyzed by Agilent
89 gas chromatography (GC) (model 7890A, Agilent Technologies, Santa Clara, CA, USA) equipped with
90 a DB-1701 column (Agilent Technologies, 30 m × 0.25 mm id, 0.25 μm). The GC parameters were the
91 following: injection temperature 275°C and FID detector temperature 300 °C; split ratio 1:50. The
92 temperature program started at 50°C and was held for 5 minutes; then the temperature was
93 increased at 10° C/min to 200°C, followed by a 10-min hold. Product separation and identification
94 were performed by Agilent GC equipped with mass spectrometry (model 5977A, Agilent
95 Technologies). The conversion of feed and the product yields were calculated on a molar basis of
96 carbon.

97

98 **Theoretical details.** All calculations were performed using the Gaussian 09 software¹⁵ with M06-2X
99 density functional and the def2TZVP basis set. We chose the M06-2X method because it was
100 suggested for broad applications on main-group thermochemistry, kinetics, and noncovalent
101 interactions.¹⁶ All structural optimizations were fully relaxed. Vibrational frequency calculations were
102 performed at the same level of theory to classify the nature of the stationary point as a minimum
103 structure and gained the thermodynamic properties at 25°C and 1 bar. To include the contributions
104 from the solvent in the reaction enthalpies (ΔH^{rxn}) and free energies (ΔG^{rxn}), the polarizable
105 continuum model¹⁷ was performed.

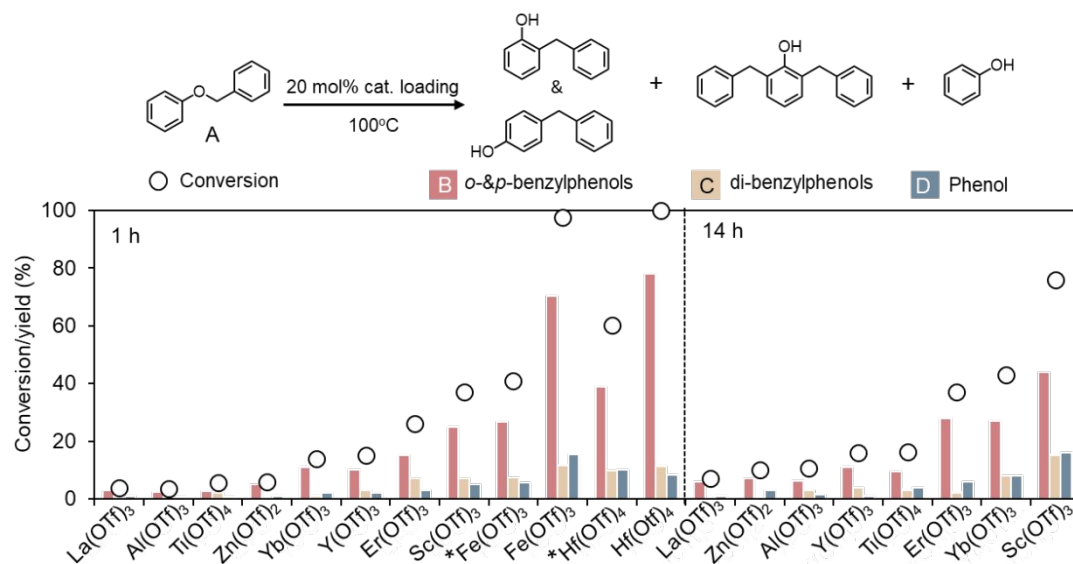
106

107 **Results**

108 ***Screening of metal triflates for conversion of benzyl phenyl ether***

109 To determine the best-performing catalyst for conversion of benzyl phenyl ether (α -O-4
110 linkage), compound **A**, we screened 10 metal triflates (La(OTf)₃, Al(OTf)₃, Ti(OTf)₄, Zn(OTf)₂,
111 Yb(OTf)₃, Y(OTf)₃, Er(OTf)₃, Sc(OTf)₃, Fe(OTf)₃, and Hf(OTf)₄) at 100°C and 1 bar (**Figure 1**). At a
112 given reaction condition (i.e., 20 mol% of catalyst, 100°C, 1 bar, and 1 h), Hf(OTf)₄ and Fe(OTf)₃
113 exhibited the highest activity with a complete conversion after 1 h. The reaction products
114 consisted of three main compounds, (i) *o*- and *p*-benzylphenols (C₁₃, compound **B**); (ii) di-

115 benzylphenols (C_{20} , compound **C**); and (iii) phenol (C_6 , compound **D**). These two triflates at 20
 116 mol% catalyst loading after 1h showed 82-89% yield of desired products, *o*- and *p*-benzylphenols (**B**)
 117 and di-benzylphenols (**C**). Next, we decreased the loading of $Hf(OTf)_4$ and $Fe(OTf)_3$ to 2 mol%
 118 and performed the same reaction at $100^\circ C$ for 1 h. Interestingly, we achieved 49% yield of
 119 desired products at 60% feed conversion under a low $Hf(OTf)_4$ loading, whereas $Fe(OTf)_3$ had 34%
 120 yield of the desired products and a lower conversion (41%) compared with $Hf(OTf)_4$ at a 2 mol%
 121 catalyst loading. The other eight metal triflates promoted significantly lower yields of the desired
 122 products at low conversions (below 40%) at 20 mol% catalyst. However, for all the experiments after
 123 1 h, the selectivity toward **B** and **C** exceeded 75% regardless of the percent conversion (**Table S3**).
 124 Further, we performed the same reaction using 20 mol% of these eight metal triflates with a longer
 125 reaction time of 14 h. We observed an increase in feed conversion and yield towards desired
 126 products compared to those at 1 h. Although all metal triflates demonstrated an enhanced
 127 feed conversion and yield of desired products at a prolonged reaction time (14h) and 20
 128 mol% catalyst loading, $Hf(OTf)_4$ had the highest conversion rate and yields of desired product
 129 at a low catalyst loading (2 mol%). These results suggested that the $Hf(OTf)_4$ was the most active
 130 and selective to C_{12} - C_{22} phenolic compounds. Thus, we used $Hf(OTf)_4$ for the rest of the studies.



131
 132 **Figure 1.** Evaluation of metal triflate catalysts for conversion of benzyl phenyl ether (A) and product
 133 yields (*o*- and *p*-benzylphenols (B), di-benzylphenols (C), and phenol (D)). Reaction conditions: feed
 134 = 0.26 mmol benzyl phenyl ether, feed/heptane/dodecane (internal standard) = 1.0:8.5:0.5

135 by weight, catalyst = 20 mol%, 100°C, 1 bar, *catalyst = 2 mol%. **Figure S1** shows the
136 representative gas chromatogram of the reaction products and their mass spectra.

137

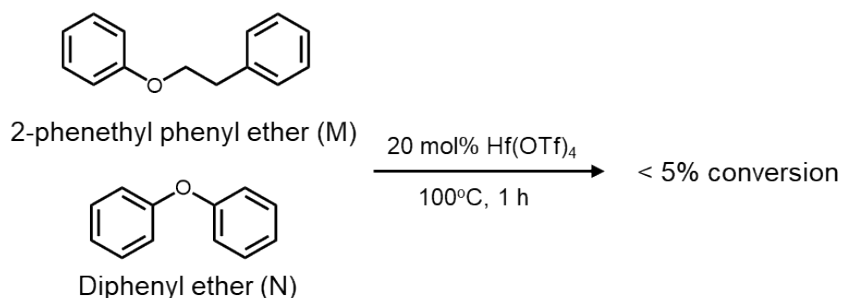
138 **Effect of chemical structure of C-O model compounds on catalytic performance**

139 To understand the effect of the chemical structure of C-O model compounds on this chemical
140 pathway, we conducted the same experiment in which we used Hf(OTf)₄ catalyst but with two other
141 model compounds, 2-phenethyl phenyl ether (compound **M** with β-O-4 linkage) and diphenyl ether
142 (compound **N** with 4-O-5 linkage) (**Figure 2**). Interestingly, Hf(OTf)₄ was essentially inactive in
143 converting 2-phenethyl phenyl ether and diphenyl ether and showed <5% conversion.

144

145 The C–O bond cleavage of 2-phenethyl phenyl ether and diphenyl ether catalyzed by Ni^{18, 19}
146 typically yields phenol and toluene as major products. However, we did not observe reaction
147 products from the conversion of 2-phenethyl phenyl ether and diphenyl ether by Hf(OTf)₄.
148 Huang et al. used Yb(OTf)₃ and more severe reaction conditions (200°C, 4h in methanol and 30 bar
149 H₂) to convert phenethyl phenyl ether; they did not observe any conversion. Yang et al. used In(OTf)₃
150 with diphenyl ether at 330°C for 1 h and observed 11% conversion.²⁰ The bond dissociation
151 energies (BDE) of the C-O bond of diphenyl ether (4-O-5) and 2-phenethyl phenyl ether (β-O-
152 4) are ~77 and 57 kcal/mol, respectively, greater than the BDE of benzyl phenyl ether (α-O-4,
153 49 kcal/mol).²¹ **Table S1** shows the relative lignin linkages content of softwood, hardwood,
154 and grass and their BDEs. We did not observe the feed conversion under our reaction
155 condition because a higher reaction temperature is required to cleave the C-O bond of these
156 two model compounds. However, the formation of benzylphenols and di-benzylphenols from
157 benzyl phenyl ether by metal triflates did not proceed by hydrolysis of the C-O cleavage.

158



159

160 **Figure 2.** Conversion of 2-phenethyl phenyl ether and diphenyl ether by $\text{Hf}(\text{OTf})_4$. Reaction
 161 conditions: feed = 0.26 mmol 2-phenethyl phenyl ether or diphenyl ether,
 162 feed/heptane/dodecane (internal standard) = 1.0:8.5:0.5 by weight, catalyst = 20 mol%,
 163 100°C, 1 bar, 1h.

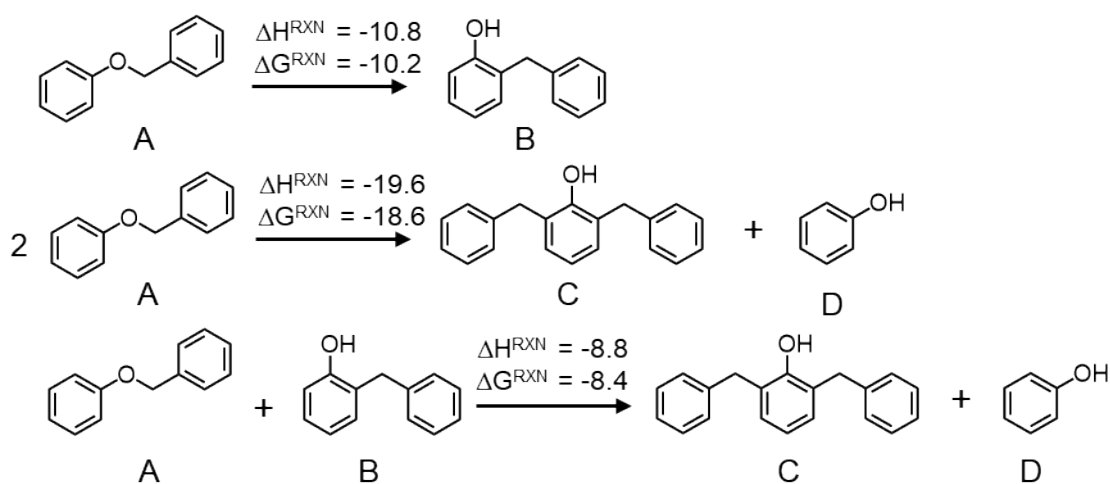
164

165 Energetics and proposed mechanism of benzyl phenyl ether transformation

166 On the basis of the resulting products, we proposed the chemical pathway shown in **Figure 3**.

167 To validate the feasibility of the cleavage of C–O bonds of benzyl phenyl ether and the formation of
 168 multi-ring precursors by C–C coupling, we determined the energetics using the M06-2X density
 169 functional and the def2TZVP basis set for the uncatalyzed reactions. These calculations suggested
 170 that the C–O breaking, and C–C coupling reactions were thermodynamically favorable (i.e., ΔG^{rxn} =
 171 -18.6 to -8.4 kcal/mol) and exothermic (i.e., ΔH^{rxn} = -19.6 to -8.8 kcal/mol) for all possible reactions.

172



173

174 **Figure 3.** Computed energetics of possible benzyl phenyl ether reactions at the M06-2X
 175 density functional and the def2TZVP basis set, 25°C, 1 bar, heptane solvent. Note that
 176 energies are in kcal/mol. Coordinates of these species are shown in the *Supplementary*
 177 *Information*.

178

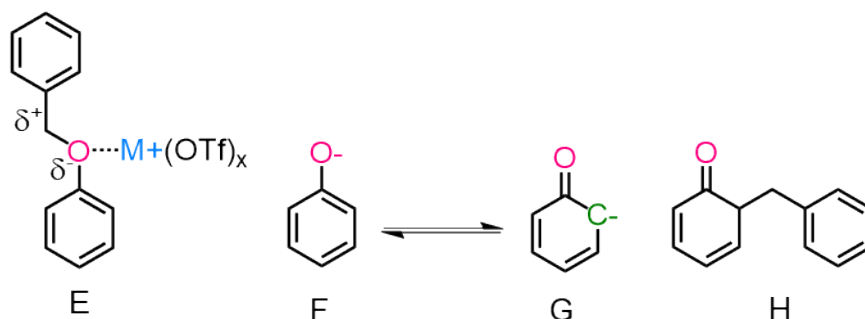
179 We proposed this mechanism based on relevant intermediates and products (**Scheme 2**). The
 180 strong Lewis acid from the metal center of metal triflates interacts with etheric oxygen (Lewis
 181 base) to form an O-aryl complexation (complex E).²² As a result, the ether bond is polarized

182 and heterolytically cleaved into a phenolated ion (intermediate **F**). Then the charge
 183 stabilization within the resonance structure of **F** leads to the formation of a carbanion
 184 (intermediate **G**) that has a negative charge at a carbon atom on the ring.²³ For the C–C
 185 coupling step, we suggest that the carbanion (**G**) reacts with complex **E** via an electrophilic
 186 attack-type mechanism to form a keto-intermediate (**H**), which is eventually tautomerized
 187 into a more stable enol-compound (benzylphenols, **B**).

188

189 In contrast, Yoon et al.⁷ used silica-alumina to catalyze the conversion of benzyl phenyl ether into
 190 benzylphenols at 100°C and 5 bar helium. However, the mechanism of the formation of
 191 benzylphenols by Brønsted acid sites was unknown. Therefore, the investigators proposed that
 192 Brønsted acid sites of silica-alumina activated the C-O cleavage and catalyzed Claisen rearrangement
 193 to produce benzylphenols. Further investigations in conjunction with the quantum calculations are
 194 needed to confirm the chemical pathway for the formation of the benzylphenols.

195



196

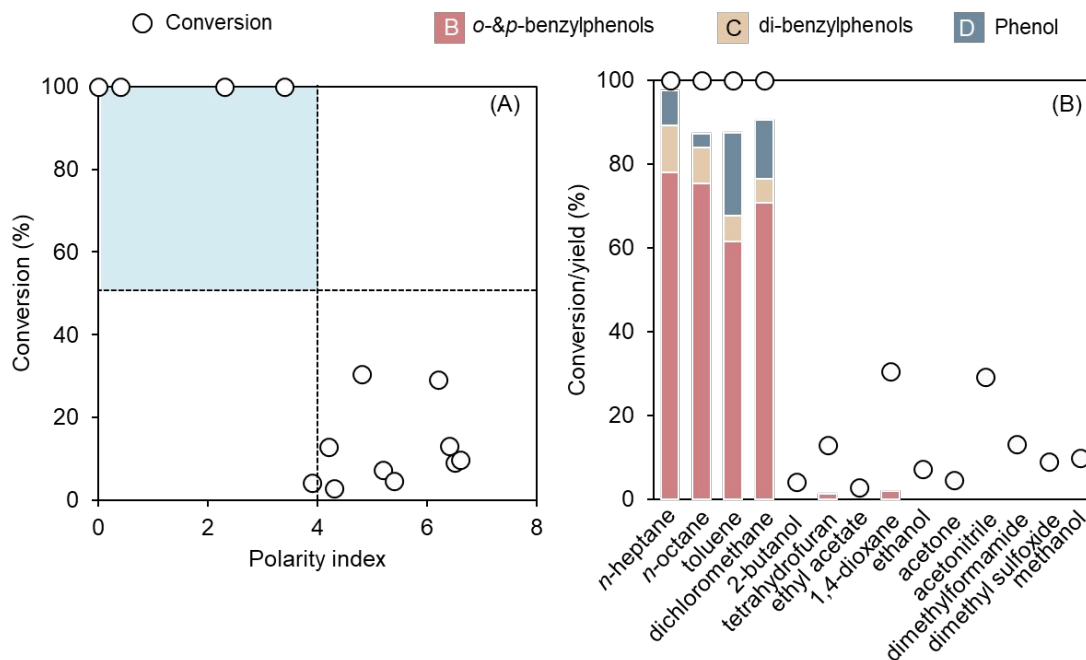
197 **Scheme 2.** The relevant intermediates in the proposed mechanism of the simultaneous C-O breaking
 198 and C-C coupling of benzyl phenyl ether.

199

200 ***Effect of solvent on product selectivity of benzyl phenyl ether transformation***

201 The solvent affects catalyst activity and product selectivity. To determine the effect of solvent
 202 polarity on the catalytic activity and product selectivity by $Hf(OTf)_4$, we varied the reaction solvents
 203 with polarity indexes from 0.0-6.6 (**Table S4**). Feed conversion by $Hf(OTf)_4$ demonstrated a strong
 204 dependence on the solvent polarity (**Figure 4A**). Relatively nonpolar solvents (i.e., *n*-heptane, *n*-
 205 octane, toluene, DCM) were active (100% conversion) and yielded >68% of desired products, *o*- and

206 *p*-benzylphenols (**B**) and di-benzylphenols (**C**) (**Figure 4B**). Interestingly, Hf(OTf)₄ became significantly
 207 less active (<31% conversion) in solvents with a polarity index greater than 3.4.
 208
 209



210
 211 **Figure 4.** Effect of solvents on the catalytic performance of hafnium triflate. (A) Conversion of benzyl
 212 phenyl ether as a function of polarity index, and (B) Feed conversion and product yield from
 213 reactions in various solvents. Reaction conditions: feed = 0.26 mmol benzyl phenyl ether,
 214 feed/solvent/dodecane (internal standard)) = 1.0:8.5:0.5 by weight, Hf(OTf)₄ = 20 mol%,
 215 100°C, 1 bar, 1h.

216

217 Discussion

218 Severe depolymerization and multiple transformation steps are the major challenges in
 219 upgrading lignin fragments.^{8, 12-14} Here, we described the conversion of benzyl phenyl ether into
 220 C₁₂-C₂₂ phenolic compounds by metal triflates. Hafnium triflate, Hf(OTf)₄, was the most active in
 221 solvents with polarity index < 3.4 and the most selective for C₁₂-C₂₂ phenolic compounds. This
 222 transformation of benzyl phenyl ether into high carbon number phenolic compounds was less
 223 complex compared with the typical depolymerization and alkylation pathways.^{9, 10}

224

225 Our most significant finding was the simultaneous C-O breaking and C-C coupling of benzyl phenyl
226 ether into high-carbon phenolics by metal triflates under a mild reaction condition (100°C and 1
227 bar). Soluble catalysts such as metal triflates react efficiently with targeted linkages, they minimize
228 competing pathways, and they enable the use of milder reaction conditions compared with solid
229 catalysts.²⁴ Although investigators used Lewis acid salts as catalysts for the C-O cleavage of lignin
230 model compounds, their focus was on the C-O cleavage into monomers. For example, Duess et al.²⁵
231 and Shen et al.²⁶ used metal triflates to catalyze the C-O cleavage of β -O-4 model
232 compounds. However, only low-carbon number guaiacol-derived products (C₆-C₉) were
233 produced. Similarly, Klein et al. used a combination of Pd/C and Lewis acid salts (Zn(OAc)₂,
234 FeCl₃, ZnCl₂) as co-catalysts to cleave β -O-4 model compounds in methanol and 35 bar H₂,
235 which promoted the hydrogenolysis and hydrogenation into a mixture of phenolic monomers
236 and their saturated analogs.²⁷ Huang et al. used a combination of metal triflates and Pd/C
237 catalyst to cleave β -O-4, α -O-4, and 4-O-5 model compounds in methanol, 30 bar H₂ at 160-
238 180°C.²⁸ Although they used the α -O-4 model compound, they did not observe the C₁₂-C₂₂
239 products because the presence of H₂ and hydrogen donor solvent (methanol) promoted
240 hydrogenolysis and hydrogenation.

241
242 The classic acid-catalyzed depolymerization of compounds with aryl ether bonds focuses on
243 the C-O cleavage and gives low yields of monomers because of condensation.²⁹ To be
244 maximally useful, subsequent C-C coupling is needed to extend the carbon number of these
245 compounds. The simultaneous C-O breaking and C-C coupling in our approach efficiently satisfy this
246 requirement. Bai et al.³⁰ used Lewis acid sites of montmorillonite catalysts to promote the alkylation
247 of phenol and benzyl acetate to produce benzylphenols at 140°C. In addition, Bi et al.¹⁰ and Zhang et
248 al.⁹ used a cascade of lignin depolymerization by HZSM-5 at 400-550°C and alkylation by an acidic
249 ionic liquid, [C₄C₁im]Cl-2AlCl₃, at 20-80°C to produce C₈-C₁₅ phenolics. Although high-carbon
250 number phenolics were generated from these processes, the addition of an alkylation step
251 requires additional catalysts and processing conditions that increase production cost.⁸
252 Instead, our process in which metal triflates catalyzed the direct C-O breaking and
253 simultaneous C-C coupling of benzyl phenyl ether (α -O-4 bond) into two- and three-ring
254 compounds eliminates any increased cost. In addition, our process suggested that the
255 molecular structure of the ether bonds is important in product formation.

256

257 Significantly, the choice of reaction solvent is important to maximize the catalytic
258 performance of the transformation of benzyl phenyl ether. We found that low polar solvents
259 with a polarity index less than 3.4 promoted catalyst activity and selectivity to desired
260 products. Lin et al.³¹ performed Fries rearrangement of aryl esters over β -zeolite at 150°C in
261 solvents of polarities in the order: *n*-decane < toluene < nitrobenzene < N-methyl-2-
262 pyrrolidone < dimethyl sulfoxide. They observed a decrease in feed conversion as a function
263 of increasing solvent polarity. Jayat et al.³² applied β -zeolite for Fries rearrangement of
264 phenyl acetate in sulfolane and dodecane as a solvent at 160°C. They found that the more
265 polar sulfolane competed with phenyl acetate for adsorption on the acid sites, a result similar
266 to our findings. Although the low-polar solvents enhanced the formation of our desired
267 products (C₁₂-C₂₂ phenolic compounds), high-polar solvents are preferred to solubilize the
268 lignin-derived phenolics and enhance the contact between feed and catalysts. Moreover,
269 these polar solvents, such as dioxane,²⁵ dimethylsulfoxide,³³ and alcohols^{27, 28} are typically
270 used to fractionate and depolymerize lignin. Thus, additional studies should focus on the
271 development of the active catalysts to produce C₁₂-C₂₂ phenolic compounds in polar solvents.
272 These C₁₂-C₂₂ phenolic compounds (benzylphenols and di-benzylphenol products) have shown
273 potential applications for phenolic-type polymers (phenol-formaldehyde resins),³⁴ diesel and jet fuel
274 precursors,^{7, 8} and liquid organic hydrogen carriers.^{35, 36}

275

276 Although the C-O model compounds used in this study are commonly used to represent C-O
277 bonds of lignin, they lack α and γ hydroxyl groups and methoxy group substitution patterns
278 on the aromatic ring that mimic the combination of H, G, and S monomer units found in
279 natural lignin. Moreover, previous studies showed that these functionalities affect chemical
280 reactivity.^{28, 37, 38} Studies in progress focus on the synthesis of α -O-4 model compounds with
281 methoxy group substitution patterns on the aromatic ring and β -O-4 model compounds with
282 α and γ hydroxyl groups and methoxy group substitution on the aromatic ring to determine
283 the effect of these functionalities on the C-O breaking and C-C coupling.

284

285

286

287 Conclusion

288 Hafnium triflate catalyzed simultaneous C–O bond breaking and C–C bond coupling of benzyl
289 phenyl ether into the large C₁₂-C₂₂ phenolic compounds under a mild condition (100°C and 1 bar).
290 The conversion of benzyl phenyl ether and selectivity to desired products increased with decreasing
291 polarity of solvents. Although we showed the potential of hafnium triflate to catalyze the direct C-O
292 cleavage and C-C coupling of benzyl phenyl ether into C₁₂-C₂₂ phenolics, a few questions remain. We
293 are currently assessing the effect of methoxy group substitution patterns on the aromatic ring
294 on the C-O breaking and C-C coupling of the α -O-4 model compounds; in addition, we are testing
295 catalyst reuse and the ability to apply this chemical pathway to upgrade technical lignin.

296

297 Acknowledgment

298 A portion of this material is based on work supported by the National Science Foundation under
299 Cooperative Agreement No. 1355438. This work was performed in part at the Conn Center for
300 Renewable Energy Research at the University of Louisville, which belongs to the National Science
301 Foundation NNCI KY Manufacturing and Nano Integration Node, supported by ECCS-1542174. The
302 authors would like to thank Dr. Howard Fried for his valuable comments and suggestions on the
303 manuscript.

304

305 References

- 306 1. G. W. Huber and A. Corma, *Angew. Chem. Int. Ed.*, 2007, **46**, 7184-7201.
- 307 2. J. Ma, S. Shi, X. Jia, F. Xia, H. Ma, J. Gao and J. Xu, *J. Energy Chem.*, 2019, **36**, 74-86.
- 308 3. E. Adler, *Ind. Eng. Chem.*, 1957, **49**, 1377-1383.
- 309 4. S. Guadix-Montero and M. Sankar, *Top. Catal.*, 2018, **61**, 183-198.
- 310 5. P. C. Rodrigues Pinto, E. A. Borges da Silva and A. E. Rodrigues, *Ind. Eng. Chem. Res.*, 2011,
311 **50**, 741-748.
- 312 6. W. Xu, S. J. Miller, P. K. Agrawal and C. W. Jones, *ChemSusChem*, 2012, **5**, 667-675.
- 313 7. J. Yoon, Y. Lee, J. Ryu, Y.-A. Kim, E. Park, J.-W. Choi, J.-M. Ha, D. Suh and H. Lee, *Appl. Catal.,*
314 *B*, 2013, **142**, 668-676.
- 315 8. H. Wang, H. Ruan, H. Pei, H. Wang, X. Chen, M. Tucker, J. Cort and B. Yang, *Green Chem*,
316 2015, **17**, 5131-5135.
- 317 9. Y. Zhang, P. Bi, J. Wang, P. Jiang, X. Wu, H. Xue, J. Liu, X. Zhou and Q. Li, *Appl. Energy*, 2015,
318 **150**, 128-137.
- 319 10. P. Bi, J. Wang, Y. Zhang, P. Jiang, X. Wu, J. Liu, H. Xue, T. Wang and Q. Li, *Biores Technol.*,
320 2015, **183**, 10-17.
- 321 11. C. Zhao, D. M. Camaioni and J. A. Lercher, *J. Catal.*, 2012, **288**, 92-103.
- 322 12. C. Li, X. Zhao, A. Wang, G. W. Huber and T. Zhang, *Chem. Rev.*, 2015, **115**, 11559-11624.
- 323 13. K. Sanderson, *Nature*, 2011, **474**, S12-S14.

- 324 14. X. Cui, H. Yuan, K. Junge, C. Topf, M. Beller and F. Shi, *Green Chem.*, 2017, **19**, 305-310.
- 325 15. M. Frisch, G. Trucks, H. Schlegel, G. Scuseria, M. Robb, J. Cheeseman, G. Scalmani, V. Barone,
326 B. Mennucci, G. Petersson, H. Nakatsuji, M. Caricato, X. Li, H. Hratchian, A. Izmaylov, J.
327 Bloino, G. Zheng, J. Sonnenberg, M. Hada, M. Ehara, K. Toyota, R. Fukuda, J. Hasegawa, M.
328 Ishida, T. Nakajima, Y. Honda, O. Kitao, H. Nakai, T. Vreven, J. Montgomery, J. Peralta, F.
329 Ogliaro, M. Bearpark, J. Heyd, E. Brothers, K. Kudin, V. Staroverov, R. Kobayashi, J. Normand,
330 K. Raghavachari, A. Rendell, J. Burant, S. Iyengar, J. Tomasi, M. Cossi, N. Rega, J. Millam, M.
331 Klene, J. Knox, J. Cross, V. Bakken, C. Adamo, J. Jaramillo, R. Gomperts, R. Stratmann, O.
332 Yazyev, A. Austin, R. Cammi, C. Pomelli, J. Ochterski, R. Martin, K. Morokuma, V. Zakrzewski,
333 G. Voth, P. Salvador, J. Dannenberg, S. Dapprich, A. Daniels, Ö. Farkas, J. Foresman, J. Ortiz, J.
334 Cioslowski and D. Fox, 2008.
- 335 16. Y. Zhao and D. Truhlar, *Acc. Chem. Res.*, 2008, **41**, 157-167.
- 336 17. J. Tomasi, B. Mennucci and R. Cammi, *Chem. Rev.*, 2005, **105**, 2999-3094.
- 337 18. J. He, C. Zhao and J. A. Lercher, *J. Am. Chem. Soc.*, 2012, **134**, 20768-20775.
- 338 19. A. G. Sergeev and J. F. Hartwig, *Science*, 2011, **332**, 439-443.
- 339 20. L. Yang, Y. Li and P. Savage, *Ind. Eng. Chem. Res*, 2014, **53**, 2633-2639.
- 340 21. R. Parthasarathi, R. A. Romero, A. Redondo and S. Gnanakaran, *J. Phys. Chem. Lett.*, 2011, **2**,
341 2660-2666.
- 342 22. A. Bagno, W. Kantlehner, R. Kreß and G. Saielli, *Zeitschrift für Naturforschung B*, 2004, **59**,
343 386-397.
- 344 23. V. Roberts, S. Fendt, A. A. Lemonidou, X. Li and J. A. Lercher, *Appl. Catal., B*, 2010, **95**, 71-77.
- 345 24. P. Deuss, K. Barta and J. de Vries, *Catal. Sustain. Energy*, 2014, **4**, 1174-1196.
- 346 25. P. Deuss, C. Lahive, C. Lancefield, N. Westwood, P. Kamer, K. Barta and J. de Vries,
347 *ChemSusChem*, 2016, **9**, 2974 – 2981.
- 348 26. X.-j. Shen, Q. Meng, Q. Mei, H. Liu, J. Yan, J. Song, D. Tan, B. Chen, Z. Zhang and G. Yang,
349 *Chem. Sci.*, 2020, **11**, 1347-1352.
- 350 27. I. Klein, C. Marcum, H. Kenttämäa and M. M. Abu-Omar, *Green Chem.*, 2016, **18**, 2399-2405.
- 351 28. X. Huang, O. Gonzalez, J. Zhu, T. Korányi, M. Boot and E. Hensen, *Green Chem.*, 2017, **19**,
352 175-187.
- 353 29. E. Adler, *Wood Sci. Technol.*, 1977, **11**, 169-218.
- 354 30. J. Bai, Y. Zhang, X. Zhang, C. Wang and L. Ma, *ACS Sustainable Chem. Eng.*, 2021, **9**,
355 7112–7119.
- 356 31. R. Lin, S. Mitchell, T. Netscher, J. Medlock, R. Stemmler, W. Bonrath, U. Létinois and J. Pérez-
357 Ramírez, *Catal. Sci. Technol.*, 2020, **10**, 4282-4292.
- 358 32. F. Jayat, M. Picot and M. Guisnet, *Catal. Lett.*, 1996, **41**, 181-187.
- 359 33. J. Mottweiler, T. Rinesch, C. Besson, J. Buendia and C. Bolm, *Green Chem.*, 2015, **17**, 5001-
360 5008.
- 361 34. N. Dunga and N. Jumbam, *Macromol. Symp.*, 2012, **313**, 121-127.
- 362 35. P. Rao and M. Yoon, *Energies*, 2020, **13**, 6040.
- 363 36. X. Chen, C. Gierlich, S. Schötz, D. Blaumeiser, T. Bauer, J. Libuda and R. Palkovits, *ACS*
364 *Sustainable Chem. Eng.*, 2021.
- 365 37. C. Lahive, P. Kamer, C. Lancefield and P. Deuss, *ChemSusChem*, 2020, **13**, 4238.
- 366 38. M. A. Hossain, T. K. Phung, M. S. Rahaman, S. Tulaphol, J. B. Jasinski and N. Sathitsuksanoh,
367 *Appl. Catal., A*, 2019, **582**, 117100.

368